

# Delay-induced synchronization phenomena in an array of globally coupled logistic maps

A. C. Martí and C. Masoller

*Instituto de Física, Facultad de Ciencias,*

*Universidad de la República, Iguá 4225, 11400 Montevideo, Uruguay*

(Dated: February 9, 2020)

We study the synchronization of a linear array of globally coupled identical logistic maps. We consider a time-delayed coupling that takes into account the finite velocity of propagation of the interactions. We find globally synchronized states in which the elements of the array evolve along a periodic orbit of the uncoupled map, while the spatial correlation along the array is such that an individual map sees all other maps in his present, current, state. For values of the nonlinear parameter such that the uncoupled maps are chaotic, time-delayed mutual coupling suppress the chaotic behavior by stabilizing a periodic orbit which is unstable for the uncoupled maps. The stability analysis of the synchronized state allows us to calculate the range of the coupling strength in which global synchronization can be obtained.

PACS numbers: 05.45.Xt, 05.65.+b, 05.45.Ra

Keywords: Synchronization; coupled map arrays; time delays; logistic map

## I. INTRODUCTION

Coupled oscillator models are widely used to model complex dynamics in non-equilibrium extended systems, and their synchronization has attracted a lot of attention in recent years [1]. In studies of coupled ensembles of nonlinear oscillators, different situations have been considered (identical or non-identical units, periodic or chaotic single-unit behavior, local or global coupling), and a rich variety of synchronization phenomena has been found (for a recent review, see [2]).

In the field of coupled map lattices, the paradigmatic model, originally introduced by

Kaneko [3, 4], is the ensemble of  $N$  logistic maps with mean field global coupling:

$$x_i(t+1) = (1 - \epsilon)f[x_i(t)] + \frac{\epsilon}{N} \sum_{j=1}^N f[x_j(t)], \quad (1)$$

$i \in [1, N]$ ,  $f(x) = ax(1 - x)$ , and  $\epsilon$  is the coupling strength. For relatively large coupling global (full) synchronization occurs: the array synchronizes on the manifold  $x_1 = \dots = x_N$ , where the dynamics of an element is generated by the uncoupled map. For weaker coupling cluster (or partial) synchronization occurs: the array splits into  $K$  clusters of  $N_1, \dots, N_K$  elements mutually synchronized [5, 6].

A characteristic of many biological and physical systems is time-delayed coupling in the interaction among many units. In the case of globally coupled units, the introduction of time delays makes the spatial coordinates of an element relevant in spite of the infinite range of the mean-field interaction. This situation was considered in Ref.[7] for one-dimensional arrays of coupled phase oscillators. It was shown that in the limit of short delays the ensemble approaches a state of frequency synchronization, and that this state might develop a spatial nontrivial distribution of phases. In two-dimensional arrays, distance-dependent time delays induce a variety of patterns including traveling rolls, steady patterns, spirals, and targets [8].

Here we study retardation effects in a linear array of logistic maps:

$$x_i(t+1) = (1 - \epsilon)f[x_i(t)] + \frac{\epsilon}{N} \sum_{j=1}^N f[x_j(t - \tau_{ij})], \quad (2)$$

where  $\tau_{ij} = k|i - j|$  is proportional to the distance between the  $i$ th and  $j$ th maps and  $k$  is the inverse of the velocity of the signal that travels through the array. In a previous work [9] we considered the case in which the uncoupled maps evolve in a periodic orbit of period 2 (when  $3 \leq a \leq 1 + \sqrt{6}$ ). We found that for weak coupling the array divides into clusters, and the behavior of the individual elements within each cluster depend on the delay times. For strong enough coupling global synchronization occurs, where the dynamics of an element is periodic of period 2, generated by the uncoupled logistic map. The spatial correlation of the elements along the array is such that if  $k$  is even, at time  $t$  all elements are in the same state, while if  $k$  is odd, at time  $t$  neighboring elements are in different states. In both cases an individual map sees all other maps in his present, current, state.

In this paper we extend the previous study and consider that the uncoupled maps can be either periodic or chaotic (i.e.,  $3 \leq a \leq 4$ ). We find that for adequate coupling strength and

time delay, global synchronization occurs. In the globally synchronized state all elements evolve along a periodic orbit of the uncoupled logistic map. Remarkably, this orbit might be unstable for the uncoupled maps. In particular, when the uncoupled maps are chaotic, time-delayed coupling might suppress chaos, stabilizing an unstable periodic orbit. For small arrays we study the stability of the globally synchronized solution and calculate the minimum coupling strength above which the unstable orbit of the uncoupled maps becomes stable for the time-delayed coupled maps. The numerical simulations are in excellent agreement with the stability analysis.

This paper is organized as follows. In Sec. II we analyze the existence and the stability of the globally synchronized state. In Sec. III we present results of the numerical simulations and the stability analysis. Finally, in Sec. IV we present a summary and the conclusions.

## II. GLOBALLY SYNCHRONIZED SOLUTIONS

A special class of solutions of Eq. (2) is characterized by the fact that, for all pairs  $i, j$ , the signal received by map  $i$  at each time corresponds to a *delayed* state of map  $j$  that coincides with the *present* state of map  $i$ :

$$x_j(t - \tau_{ij}) = x_i(t). \quad (3)$$

Thus, each element “perceives” the array as being fully synchronized, in spite of the fact that the simultaneous states of different elements might not coincide. In these globally synchronized solutions each element evolves along a limit cycle of period  $P$  of the uncoupled logistic map with a given phase, such that we can write

$$x_i(t) = x_0(t + \phi_i) \quad (4)$$

with  $x_0(t)$  a particular realization of the limit cycle, used as a reference orbit. The condition for this solution to satisfy the evolution equation is

$$\phi_i - \phi_j + m_{ij}P = \tau_{ij} = k|i - j| \quad (5)$$

for all  $i$  and  $j$ , where  $m_{ij}$  are arbitrary integer numbers. The symmetry of the delays,  $\tau_{ij} = \tau_{ji}$ , implies that

$$\phi_i - \phi_j + m_{ij}P = \phi_j - \phi_i + m_{ji}P. \quad (6)$$

Thus, the phase differences  $\phi_i - \phi_j$  cannot be arbitrary but have to be either  $\phi_i - \phi_j = n_{ij}P$ , or  $\phi_i - \phi_j = P/2 + n_{ij}P$ , with  $n_{ij}$  an integer number.

We shall refer to solutions with  $\mod(\phi_i - \phi_j, P) = 0 \forall i$  and  $j$  as *in-phase* solutions, and solutions with  $\mod(\phi_{i+1} - \phi_i, P) = P/2 \forall i$  as *anti-phase* solutions. Since  $\mod(\phi_{i+1} - \phi_i, P)$  is an integer number, the period  $P$  of the orbit for the anti-phase solution has to be even. The in-phase and anti-phase solutions verify Eq. (5) only for certain delay times. For the in-phase solution,

$$\mod(\phi_i - \phi_j, P) = \mod(k|i - j|, P) = 0 \quad (7)$$

$\forall i$  and  $j$  only if  $k = nP$  with  $n$  an integer number; for the anti-phase solution,

$$\mod(\phi_{i+1} - \phi_i, P) = \mod(k, P) = P/2 \quad (8)$$

only if  $k = P/2 + nP$  with  $n$  an integer number.

The existence of these globally synchronized states is independent of the coupling strength; the only requirement is that the periodic orbit is a solution (stable or unstable) of the logistic map.

To analyze the stability of the globally synchronized solutions we turn the delayed Eq. (2) into a non-delayed equation by the introduction of auxiliary variables:

$$y_{im}(t) = x_i(t - m) \quad (9)$$

where  $1 \leq i \leq N$  and  $0 \leq m \leq M$  with  $M = \max(\tau_{ij})$ . In terms of these new variables Eq. (2) becomes

$$\begin{aligned} y_{i0}(t+1) &= (1 - \epsilon)f[y_{i0}(t)] + \frac{\epsilon}{N} \sum_j^N f[y_{j,|j-i|}(t)] \\ y_{im}(t+1) &= y_{i,m-1}(t) \text{ for } m \neq 0 \end{aligned} \quad (10)$$

Next we define the vector

$$Z = (y_{10}, y_{20}, \dots, y_{N0}; y_{11}, y_{21}, \dots, y_{N1}; \dots; y_{1M}, y_{2M}, \dots, y_{NM}) \quad (11)$$

which has  $N(M + 1)$  components. The anti-phase solutions of period 2 can be written as

$$Z_A^1 = (x_a, x_b, \dots; x_b, x_a, \dots), \quad Z_A^2 = (x_b, x_a, \dots; x_a, x_b, \dots) \quad (12)$$

and the in-phase solutions of period 2 as

$$Z_I^1 = (x_a, x_a, \dots; x_b, x_b, \dots), \quad Z_I^2 = (x_b, x_b, \dots; x_a, x_a, \dots) \quad (13)$$

where  $x_a$  and  $x_b$  are the points of the period 2 orbit of the logistic map. We re-write Eq. (7) as

$$z_i(t+1) = F_i[z_1(t), \dots, z_{N(M+1)}(t)] \quad (14)$$

The in-phase and anti-phase solutions are fixed points of  $F^2$ :

$$F(F(Z_{I,A}^{1,2})) = F(Z_{I,A}^{2,1}) = Z_{I,A}^{1,2}. \quad (15)$$

To analyze the stability of these solutions we need to calculate the eigenvalues of the matrix

$$A_{ij} = \frac{\partial F_i}{\partial z_k} \Big|_{Z=Z_{I,A}^2} \frac{\partial F_k}{\partial z_j} \Big|_{Z=Z_{I,A}^1} \quad (16)$$

This matrix has  $N^2(M+1)^2$  elements which are either 1, 0,  $[1 - (N-1)\epsilon/N]f'(x_{a,b})$  or  $\epsilon/Nf'(x_{a,b})$ . Even for a small array size there is a large number of variables involved and the eigenvalues have to be calculated numerically.

### III. RESULTS

In this section we present numerical simulations and results of the stability analysis, that demonstrate global synchronization in the in-phase and anti-phase solutions discussed in the previous section. The stability analysis can only be done for small arrays and small delay times, since the size of the matrix  $A$  [Eq. (13)] increases as  $kN^2$ . For large arrays and/or large delays, we simulate the equation (2). To solve the delay equation (2) we need to specify the evolution of  $x_i(t)$  at times  $1 \leq t \leq \max(\tau_{ij})$ . We evaluated this by taking  $x_i(1)$  a random number ranging from 0 to 1 and by letting the array evolve initially without coupling.

First, we show results for the anti-phase solution, which exists for  $k$  even. For  $k = 1$ , we find that for all values of  $a$  there is a value of  $\epsilon$  above which the anti-phase solution of period 2 is stable. Figure 1 shows the absolute value of the maximum eigenvalue,  $|\lambda_{max}|$ , as a function of  $\epsilon$ , for an array of  $N = 12$  maps and three different values of the parameter  $a$ . For  $a = 3.5$  (dot-dashed line) the maps without coupling evolve in a limit cycle of period

4, for  $a = 3.83$  (dashed line) the maps without coupling evolve in a limit cycle of period 3, and for  $a = 4$  (solid line) the maps without coupling are chaotic. For clarity the dotted line indicates the stability boundary  $|\lambda_{max}| = 1$ . In the three cases, for large enough coupling the anti-phase solution of period 2 is stable ( $|\lambda_{max}| < 1$ ). Notice that the coupling strength above which the solution is stable increases with  $a$ .

We verified numerically that for larger arrays the anti-phase solution is stable. Figure 2(a) displays, as an example, a bifurcation diagram for  $N = 50$  ( $a = 4$  and  $k = 1$ ). The bifurcation diagram is done in the following way: we chose the same initial condition for all values of  $\epsilon$ , and we plot the 100 time-consecutive values  $x_i(t)$  (with  $t$  large enough) for a given element  $i$  of the array. Figure 2(b) displays the same but for a neighboring element. Above a certain coupling strength the array synchronizes in the period 2 orbit of the uncoupled map and the bifurcation diagram for the two elements coincide. The synchronization in the period 2 orbit is surprising since for  $a = 4$  the period 2 orbit is unstable for the uncoupled maps. While the anti-phase solution is stable for  $\epsilon \geq 0.6$  (see Fig. 1), Fig. 2 shows that the array synchronizes in this solution for a slightly larger coupling strength ( $\epsilon \sim 0.7$ ). The critical coupling strength,  $\epsilon_{crit}$ , above which global synchronization occurs depends slightly on the initial condition, and increases with  $a$  and  $N$ . Figure 3 displays the critical value of  $\epsilon$  (calculated averaging over 100 different initial conditions) vs.  $a$ .  $\epsilon_{crit}$  increases linearly in the parameter region where the uncoupled maps are periodic, and abruptly in the parameter region where the uncoupled maps are chaotic. Figure 4 (solid line) shows that  $\epsilon_{crit}$  also increases with the system size  $N$ .

Notice that below the critical coupling strength,  $\epsilon_{crit}$ , the bifurcation diagrams shown in Figs. 2(a) and 2(b) differ. This is due to the fact that for  $\epsilon < \epsilon_{crit}$  the array splits into a complex clustered structure. The clustering behavior in the simpler case when the uncoupled maps evolve in a period 2 orbit was studied in [9].

For larger time delays and  $k$  odd, the interval of coupling strength in which the anti-phase solution of period 2 is stable becomes more narrow. As an example, Fig. 5 displays  $|\lambda_{max}|$  vs  $\epsilon$  for  $a = 3.5$  and  $k = 1, 3, 5$ , and 7. Note that in a wide range of coupling strength  $|\lambda_{max}|$  is slightly larger than 1. In this parameter region, starting from random initial conditions there is a transient time in which the array approaches the anti-phase solution; after this transient the array exhibits a complex spatio-temporal behavior. The transient time increases with  $N$ ; as an example, Fig. 6 displays the mean value,  $\langle x \rangle = \sum_{i=1}^N x_i$ , vs. time, for four

different system sizes. The study of this unexpected effect of the system size is the object of future work.

Next, we show results for the in-phase solution, which exists for  $k = nP$ . Figure 7 displays the bifurcation diagram for two elements of the array, and  $a = 3.5$ ,  $k = 4$ , and  $N = 50$  (for  $a = 3.5$  the uncoupled maps evolve in a orbit of period 4). We observe that above a critical coupling strength ( $\epsilon_{crit} \sim 0.23$ ) the array synchronizes in the period 4 orbit of the uncoupled map. As in the case of the anti-phase solution, for coupling strengths below  $\epsilon_{crit}$  the bifurcation diagrams shown in Figs. 7(a) and 7(b), differ. This is due to the fact that the two elements belong to different clusters. The dashed line in Fig. 4 shows that  $\epsilon_{crit}$  increases with the system size  $N$ .

For arbitrary values of  $k$ ,  $a$ , and  $\epsilon$  we found a rich variety of complex spatiotemporal behaviors. The characterization of the different dynamic regimes is the object of future work.

#### IV. SUMMARY AND CONCLUSIONS

We studied the synchronization of a linear array of identical logistic maps. We consider time-delayed mutual coupling with delay times  $\tau_{ij}$  that are proportional to the distance between the maps ( $\tau_{ij} = k|i - j|$ ). Depending on the time delays and on the coupling strength, different synchronization regimes might occur. If the coupling is weak the array usually splits into a complex clustered structure. If the coupling is large enough, global synchronization occurs. In the globally synchronized state each element of the array sees all other elements in its present state [ $x_i(t) = x_j(t - \tau_{ij}) \forall i, j$ ], and all the elements of the array evolve along a periodic orbit of the uncoupled maps. The spatial correlation along the array is either periodic or homogeneous depending on  $k$ . If  $k$  is odd the array synchronizes in anti-phase, such that the state at time  $t$  of two consecutive elements is  $x_i(t) = x_0(t)$ ,  $x_{i+1}(t) = x_0(t + P/2)$  (where  $x_0(t)$  is a particular realization of the orbit of period  $P$ , used as a reference). If  $k = nP$  the array synchronizes in in-phase, such that the state at time  $t$  is  $x_i(t) = x_0(t) \forall i$ . For parameter values such that the uncoupled maps are chaotic, mutual delayed coupling suppresses chaos rendering the evolution of the elements of the array periodic in time. Thus, an important consequence of our analysis is that delayed coupling might allow controlling a chaotic array by rendering an unstable periodic orbit of the

uncoupled maps, stable.

---

[1] A.S. Pikovsky, M.G. Rosenblum, and J. Kurths, *Synchronization-A Universal Concept in Non-linear Sciences*, Cambridge University Press, Cambridge, 2001.

[2] S. Boccaletti, J. Kurths, G. Osipov, D. L. Valladares, and C.S. Zhou, Phys. Rep. 366, 1 (2002).

[3] K. Kaneko, Phys. Rev. Lett. **63**, 219 (1989).

[4] K. Kaneko, Physica D **41**, 137 (1990).

[5] A. Pikovsky, O. Popovych, and Y. Maistrenko, Phys. Rev. Lett. **87**, 044102 (2001).

[6] A. Pikovsky Physica D (2002).

[7] D. H. Zanette, Phys. Rev. E **62**, 3167 (2000).

[8] S. O. Jeong, T. W. Ko, and H. T. Moon, Phys. Rev. Lett. **89**, 154104 (2002).

[9] C. Masoller, A. C. Martí and D. Zanette, submitted.

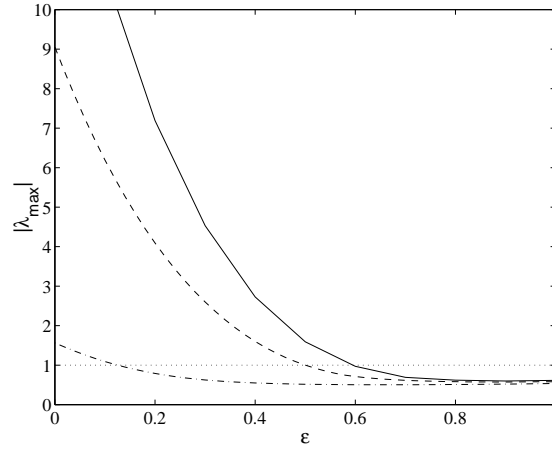


FIG. 1: Stability analysis of the anti-phase solution of period 2 for  $k = 1$  and  $N = 12$ . We plot the largest eigenvalue of the matrix  $A$  [Eq. (13)] vs. the coupling strength for  $a = 3.5$  (dot-dashed line),  $a = 3.83$  (dashed line), and  $a = 4$  (solid line).

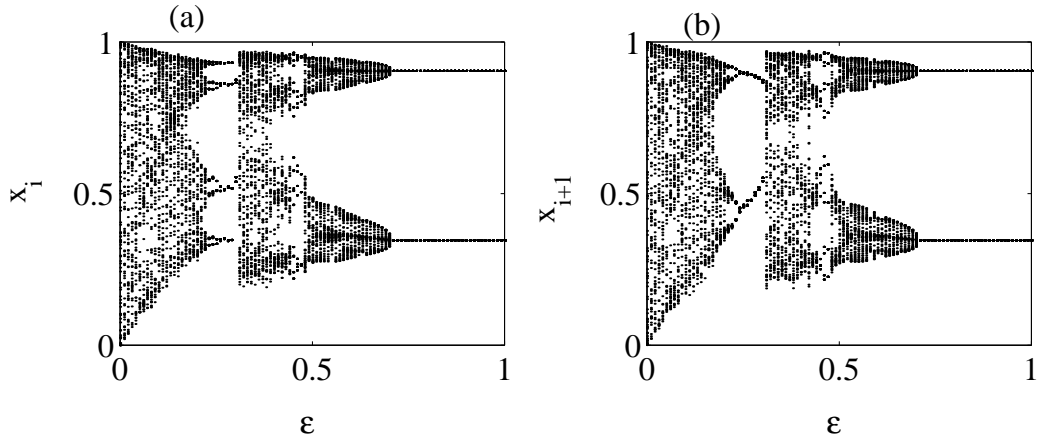


FIG. 2: Bifurcation diagram obtained numerically, integrating Eq.(2) with  $a = 4$ ,  $k = 1$ , and  $N = 50$ . We plot the values of two consecutive elements,  $x_i$  (a) and  $x_{i+1}$  (b). Notice that after a complex bifurcation scenario the two elements of the array synchronize in a period 2 orbit.

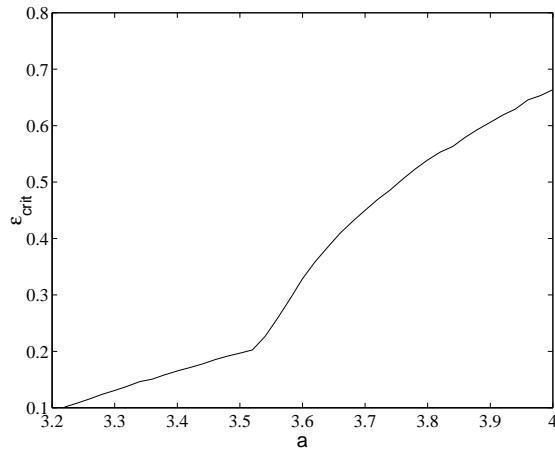


FIG. 3: Critical coupling strength above which synchronization occurs vs. the nonlinear parameter  $a$ .  $k = 1$  and  $N = 100$ .  $\epsilon_{crit}$  was calculated averaging over 100 different initial conditions.

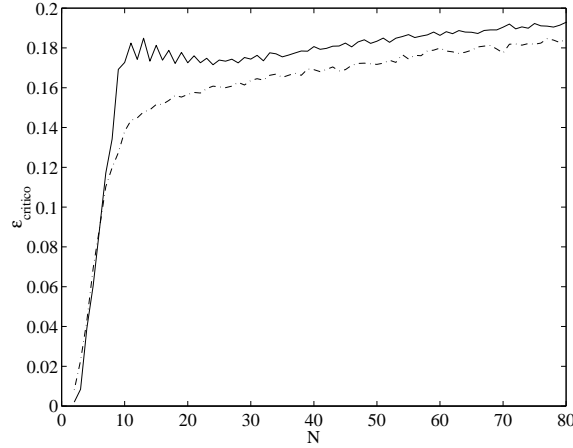


FIG. 4: Critical coupling strength above which global synchronization occurs as a function of  $N$  for  $a = 3.5$  and  $k = 1$  (solid line);  $a = 3.5$  and  $k = 4$  (dashed line).

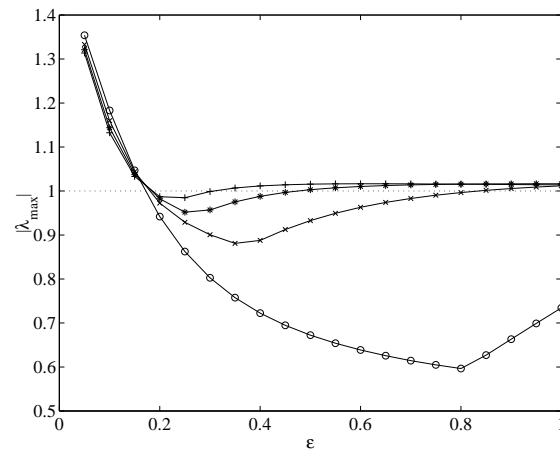


FIG. 5: Modulus of the largest eigenvalue of the matrix  $A$  as a function of  $\epsilon$  for the antiphase solution and  $a = 3.5$ ,  $k = 1$  (o),  $k = 3$  (x),  $k = 5$  (\*), and  $k = 7$  (+).

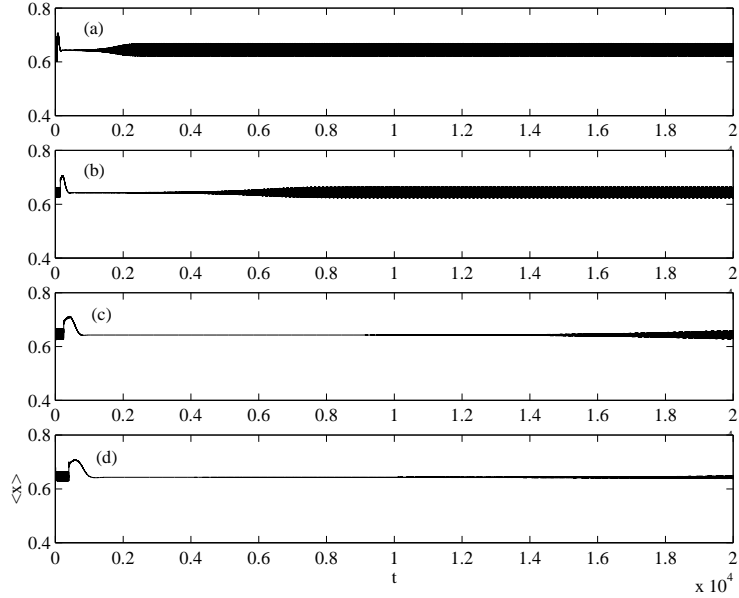


FIG. 6: Temporal evolution of the mean value  $\langle x_i(t) \rangle$  for four different system sizes,  $N = 12$  (a),  $N = 30$  (b),  $N = 50$  (c) and  $N = 80$  (d). The parameters are  $a = 3.5$ ,  $k = 5$ , and  $\epsilon = 0.6$

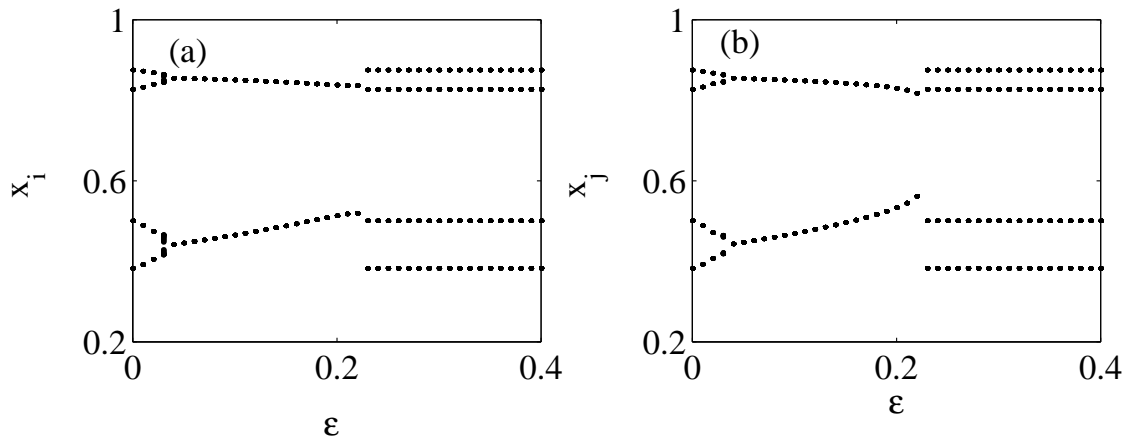


FIG. 7: Bifurcation diagram obtained numerically, integrating Eq.(2) with  $a = 3.5$ ,  $k = 4$ , and  $N = 50$ . We plot the values of two different elements of the array,  $x_i$  (a) and  $x_j$  (b). Notice that after a period-halving bifurcation the elements of the array synchronize in a period 4 orbit.